EARTH SURFACE PROCESSES AND LANDFORMS
Earth Surf. Process. Landforms **38**, 1851–1868 (2013)

Published online 13 June 2013 in Wiley Online Library
(wileyonlinelibrary.com) DOI: 10.1002/esp.3432

Decadal and seasonal development of embryo dunes on an accreting macrotidal beach: North Lincolnshire, UK

Anne-Lise Montreuil,[1] Joanna E. Bullard,[1]* Jim H. Chandler[2] and Jon Millett[1]
[1] Department of Geography, Loughborough University, Loughborough, Leicestershire UK
[2] School of Civil and Building Engineering, Loughborough University, Loughborough, Leicestershire UK

Received 2 September 2012; Revised 17 April 2013; Accepted 19 April 2013

*Correspondence to: Joanna E. Bullard, Department of Geography, Loughborough University, Leicestershire, LE11 3TU, UK. E-mail: j.e.bullard@lboro.ac.uk

ESPL
Earth Surface Processes and Landforms

ABSTRACT: Embryo dunes are often ephemeral, but can develop to become established coastal foredunes. In 2001 a patch of embryo dunes 13.11 m^2 appeared on a beach in north Lincolnshire, UK and had expanded to over 3600 m^2 by 2011. The rate of expansion is linked to storm occurrence, where expansion is slowed during years with a higher incidence of storm surges. From July 2009–October 2010 seasonal changes in dune field topography were determined using terrestrial laser scanning (TLS) data. Vegetation is important in the development of embryo dunes, but can cause errors in TLS data. Tests evaluating the impact of vegetation on the TLS data suggest the minimum elevation value from the TLS point cloud within a 0.05 m grid cell gives a good approximation of the ground surface. Digital elevation models (DEMs) of the dunes constructed using filtered data showed the embryo dunes underwent a classic seasonal cycle of erosion during the winter and accretion during the summer. For example from October 2009 to April 2010 over 375 m^3 of sediment was eroded from the dunes whereas during spring and summer 2010 the dune field gained over 600 m^3 of sand. The overall magnitude of change in dune height and volume from season to season exceeded the errors associated with the construction of the DEM from the TLS data and the vegetation filtering process, which suggests TLS can be useful for documenting topographic change in vegetated dunes. After 10 years, the patch of embryo dunes is still expanding but has not yet merged with more established foredunes to landward. Aeolian process measurements indicate that, at present, the embryo dunes do not prevent sand from reaching the foredunes, however the rate of foredune progradation has slowed concurrently with the expansion of the embryo dune field. Copyright © 2013 John Wiley & Sons, Ltd.

KEYWORDS: embryo dunes; terrestrial laser scanner; vegetation; sand budget; macrotidal beach

Introduction

Coastal embryo dunes and foredunes are dynamic landforms that develop at the marine–terrestrial–atmosphere interface (Pye, 1983; Hesp, 2011). These dunes form in a wide range of situations and environments, but are integrally-coupled to the adjacent beach and are best developed on macrotidal, dissipative beaches (Sherman and Bauer, 1993), where potential aeolian sediment supply is high and the likelihood of destruction by wave processes is moderate to low. This paper focuses on embryo dunes (also known as incipient foredunes) which are formed at the coast when wind-blown sand accumulates around an irregularity or obstacle; they are typically small (< 2 m height) and discrete and are colonized by pioneer plants such as sand couch (*Elytrigia juncea*), lyme grass (*Leymus arenarius*) and other species tolerant of seawater inundation. They can form very rapidly (e.g. Gomes *et al.*, 1992), are often unstable and can be very short-lived, removed by high tides and storm waves (Carter *et al.*, 1990; Hesp, 2002; Olivier and Garland, 2003; Suanez *et al.*, 2012) as well as being vulnerable to damage from trampling and vehicles (Pye and Blott, 2008). Given sufficient aeolian sand supply and ongoing colonization by vegetation, embryo dunes can grow in size and height becoming more resistant to overwashing and forming the basis for the development of established foredunes (Hesp, 2002). Concomitant with this is a change in the dominant species to plants such as marram grass (*Ammophila arenaria*) which are less tolerant of inundation.

The main differences between embryo dunes and established foredunes are the degree of geomorphological development (e.g. height, width, continuity) and the characteristics of the vegetation cover (Hesp, 2002, 2011). As embryo dunes are typically lower and less continuous than established foredunes and have a partial and/or seasonal vegetation cover, they are susceptible to both wind and water erosion which may lead to total destruction. Established foredunes, which are taller, wider and colonized by perennial and often woody plant species (e.g. *Lotus corniculatus*, *Salix* spp., *Ulex europaeus*), are more permanent and consequently more mature landforms. Where both embryo dunes and established foredunes occur together, the former offers some protection against marine erosion acting as a buffer between the sea and the main foredune (Carter *et al.*, 1990; Suanez *et al.*, 2012). Stages in the development from incipient to established foredunes have been described by, amongst others, Carter (1988), Arens (1994), Hesp (2002) and Mathew

et al. (2010). Hesp (2002) argues that foredunes may remain in a single state, progress through an evolutionary sequence, or in some instances progression may be reversed, for example due to erosion. When embryo dunes are able to persist long enough to evolve in to taller established foredunes, they are typically only affected by marine processes on the seaward side, as overwash and storm surges over the crest of the dune become less likely (Carter *et al.*, 1990).

Sediment supply to embryo dunes is both seasonally and annually variable, dependent on the transport capacity and direction of the wind (Olivier and Garland, 2003; Ruz and Meur-Férec, 2004; Anthony *et al.*, 2007; Suanez *et al.*, 2012). Most studies of aeolian sediment transport and airflow over coastal dunes have concentrated on foredunes – the development of incipient foredunes or embryo dunes reduces, but does not necessarily prevent onshore transport to the landward, established foredunes (e.g. Petersen *et al.*, 2011). Offshore winds can also contribute to dune development (Bauer *et al.*, 2012) and may transfer sediment from the main foredune to the embryo dune or upper beach. Other variables affecting sand supply are effective beach source width (McLean and Shen, 2006) and sediment availability, which is typically moderated by moisture content (Delgado-Fernandez, 2011) and seasonal snow and ice cover (Davidson-Arnott and Law, 1990). The effective beach width on macrotidal beaches is often large and an additional controlling factor can be the existence of intertidal bars (ridge and runnel systems), which can segment the dry fetch on the beach, trapping sand and reducing sand supply from the beach to the dunes (Anthony *et al.*, 2009). Aagaard *et al.* (2004) found that onshore migration of intertidal bars that resulted in bar welding, widening the beach, led to a substantial increase in foredune sediment supply. Thus, in addition to seasonal changes in variables such as wind regime and moisture content, seasonal variation in the number, position and migration of intertidal bars can also be important in sediment supply to the dunes. Such seasonal variability in sediment supply affects the time taken for embryo dunes to develop in to established foredunes; the other major factor is the magnitude and frequency of storm events. Partial destruction of embryo dunes during storms can slow the rate of vegetation succession (van Tooren, *et al.*, 1983), and vegetation removal and alterations to topography by erosion (e.g. scarping) will affect airflow over the dunes (Hesp, 2002). This means the transition from embryo dunes to a continuous, established foredune can take a long time, typically decades (McLean and Shen, 2006, Mathew *et al.*, 2010).

This paper assesses the factors contributing to the development of a field of embryo dunes on the east coast of England over a decade, and explores the seasonal changes in dune sediment budget over one year. The seasonal changes were captured using terrestrial laser scanning, and the usefulness of such a technique on vegetated dunes is assessed. The dunes first appeared in 2001 and their spatial extent has increased in size, but to date the dunes remain separated from pre-existing established foredunes on their landward side by the upper beach.

Study Site

Theddlethorpe beach (Lincolnshire coast, eastern England) is a dissipative macrotidal beach extending 500 m from the foredune toe to the mean low water mark. The mean spring and neap tidal ranges are 6 m and 2.86 m, respectively. The lower beach is characterized by multiple intertidal bars; typically 3–5 bars are present and although some cross-shore movement of bar crests has been observed, the dominant morphological behaviour over annual timescales is longshore migration in response to north-easterly winds (van Houwelingen *et al.*, 2006) (Figure 1). Behind the beach are well-established, accreting and regular foredunes *c.* 50–100 m wide with a height of *c.* 8 m above Ordnance Datum Newlyn (ODN; mean sea level). Comparison of historic maps and aerial photographs has shown that the annual rate of seaward advance of the main coastal foredune has been, on average, 2 m over the last 120 years (Montreuil and Bullard, 2012). In 2001 a field of vegetated embryo dunes formed on the upper beach. There were no embryo dunes visible on aerial photographs from 1953 to 2000 and it is not known what triggered their initiation during the time between the 2000 aerial photograph and that taken in 2001 where they are clearly present. Since then the embryo dunes have persisted and expanded to form a dune field that extends 265 m in the NW-SE longshore dimension, and 70 m cross-shore but remains separated from the main foredunes by an unvegetated beach which floods at high tide and varies in width from 1 m in the south to approximately 40 m in the north (2011). These dunes have formed on the beach, some distance from the main foredunes and they do not have the typical ramp, terrace or ridge forms of most incipient foredunes (Hesp, 2002), but geomorphologically resemble a cluster of shadow-type dunes that form in the lee of discrete vegetation patches (e.g. Type 1a in Hesp's 1989 classification). The embryo dunes are anchored by the grass *Elytrigia juncea* (sand couch). The beach and embryo dunes are composed of fine to medium, well to very well-sorted quartz sand (D_{50} = 253–261 μm). The main sources of sand on this coast are longshore transport of material eroded from the Holderness cliffs to the north (Figure 1a) and nearshore and subtidal sand banks (Robinson, 1964; Leggett *et al.*, 1998; Montreuil and Bullard, 2012).

The mean orientation of Theddlethorpe beach is 340°N. Along this coast, the prevailing winds are offshore from the southwest. Easterly onshore winds occur with less frequency but higher magnitude than offshore winds. In summer months winds are typically from the southwest or northeast (onshore winds) and are weaker than those in winter which mainly blow from the southwest. Under northeast winds, the wind fetch distance is more than 300 m across the beach and thus oblique onshore winds can induce high sand transport to the dunes. The coast is exposed to fetch-limited, low-energy waves in the North Sea. Although storm surge activity is low, winter storms often exceed 0.5 m of surge above high tide (van Houwelingen *et al.*, 2006). Climate in the region is temperate oceanic with a mean annual temperature of 10.4 °C and rainfall of 641 mm.

Methodology

Annual aerial photographs from 2001 to 2011, taken during summer months (usually early August), were geo-rectified to the British National Grid (OSGB36) reference system using a series of ground control points as described by Montreuil and Bullard (2012). From these, the spatial extent of the embryo dune field was digitized using ArcView 9.3 software to document annual changes. The highest astronomical tide (HAT) level, which coincides with the seaward limit of the vegetated, established coastal foredunes, was used to determine the coastline on each aerial photograph. The Digital Shoreline Analysis System (DSAS; Thieler *et al.*, 2009; Brooks and Spencer, 2010) was used in combination with ArcView to determine changes in coastline position (edge of the seaward foredunes) and changes in the distance between the coastline and the landward margin of the embryo dune field from 2001

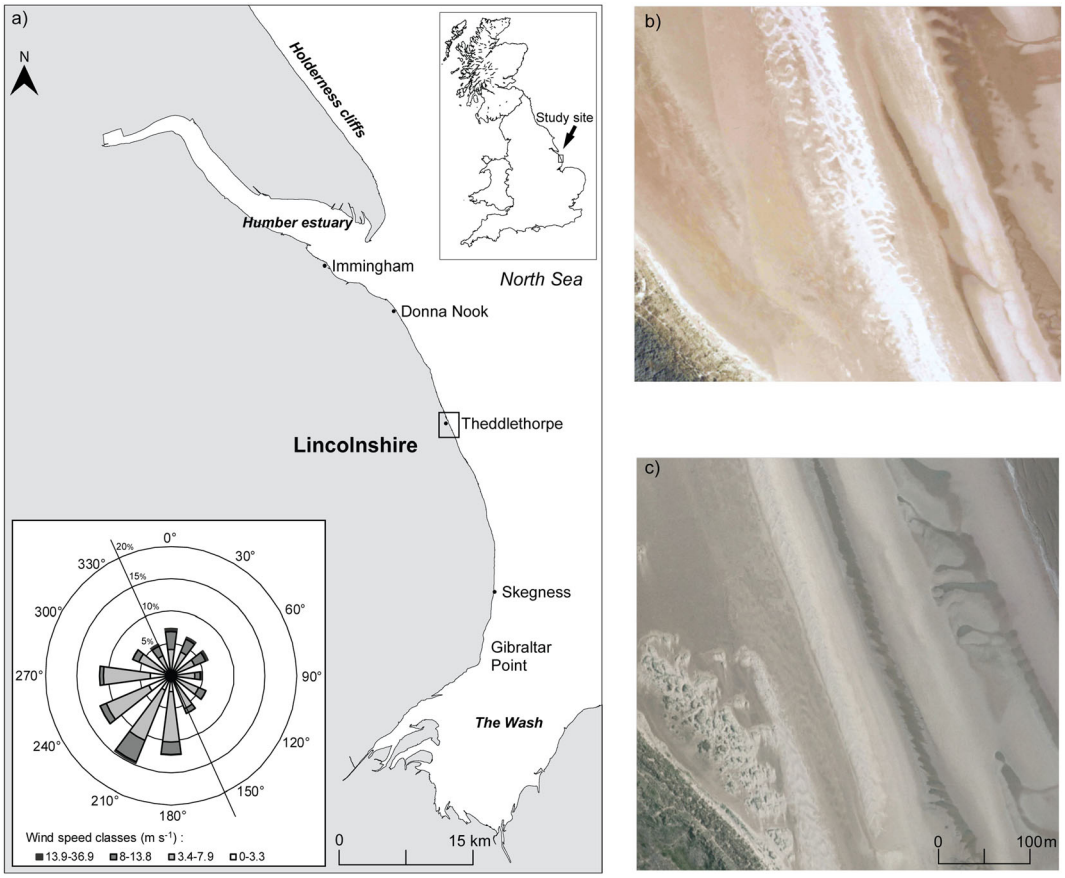

Figure 1. Study area. (a) Map of the study site; inset: annual wind rose in 2009–2011; where the line corresponds to the mean orientation of the coastline. Aerial photographs in (b) 2000 and (c) 2011. This figure is available in colour online at wileyonlinelibrary.com/journal/espl

to 2011. Using DSAS, five transects were generated that crossed the dune field perpendicular to the coastline.

Airborne and terrestrial laser scan surveys

Airborne and terrestrial laser scanning are increasingly being used to obtain high resolution topographic data in coastal and aeolian landscapes (e.g. Nagihara *et al.*, 2004; Rosser *et al.*, 2005; van Houwelingen *et al.*, 2006; Houser and Mathew, 2011; Allen *et al.*, 2012). Such data are most reliable where the ground surface to be scanned is unvegetated, such as on beaches and unvegetated dunes, because the vegetation canopy can intercept the laser leading to errors (e.g. Rango *et al.*, 2000; Coveney and Fotheringham, 2011). This interception has, however, been exploited by some researchers to provide useful information concerning the density, surface roughness and structure of the vegetation (e.g. Estornell *et al.*, 2012; Weligepolage *et al.*, 2012). In areas of less dense vegetation, attempts have been made to differentiate the vegetation and surface elevation signals using filters (Guarnieri *et al.*, 2009), but this is not possible where the vegetation canopy can not be penetrated (Rosso *et al.*, 2006) and can also be difficult in areas of variable relief.

For a previous study (Montreuil and Bullard, 2010), airborne LiDAR (light detecting and ranging) data covering the study site were obtained from the Environment Agency of England and Wales for 2001 and 2007 (at a resolution of 2 m and 1 m, respectively). The LiDAR data had been post-processed to separate the vegetation signal from the surface signal and hence represent the 'bare earth' topography. The reported accuracies range from 0.05 to 0.15 m in the vertical dimension and from 0.25 to 2 m in the horizontal dimension. These data are used here to provide an indication of the three-dimensional changes in the embryo dunes above ODN between 2001 and 2007. To quantify seasonal changes in the shape and sediment budget of the embryo dunes terrestrial laser scanning (TLS) of a small section of the dune field was undertaken. TLS has the advantage of being relatively easy to deploy over small areas and has been successfully used in previous studies to determine variation in the volume of unvegetated and sparsely-vegetated aeolian dunes, including defining areas of erosion and deposition (Nagihara *et al.*, 2004; Juraidi *et al.*, 2010). The main challenge in using TLS to determine reliable estimates of sediment budget at this site is the fact that the shape and persistence of the embryo dunes is intimately-associated with vegetation.

TLS data collection

A terrestrial laser scanner (Leica ScanStation2, Switzerland) was used to carry out surveys of the embryo dunes on 1 July 2009, 8 October 2009, 21 January 2010, 22 April 2010, 29 June 2010 and 20 October 2010 to determine seasonal topographic variation. This terrestrial laser scanner enables rapid acquisition (up to 50 000 points per second) of high resolution three-dimensional topographic data over a distance of 100 m, and can measure positions with 6 mm accuracy (Leica Geosystems, 2008) and at a ground resolution of up to 1 mm. The output of the TLS scans is a set of high resolution point clouds defined by *x*, *y*, *z* coordinates. For each survey, the embryo dune field was fully surveyed with two main acquisition scans, one from the top of the foredune (TLS 1) and the second from the middle-beach berm (TLS 2) to collect data uniformly across the site (Figure 2). To facilitate sweeps of the scanning area and to reduce the shadowing effects of the embryo dunes, the scanner was mounted on a tripod at *c.*

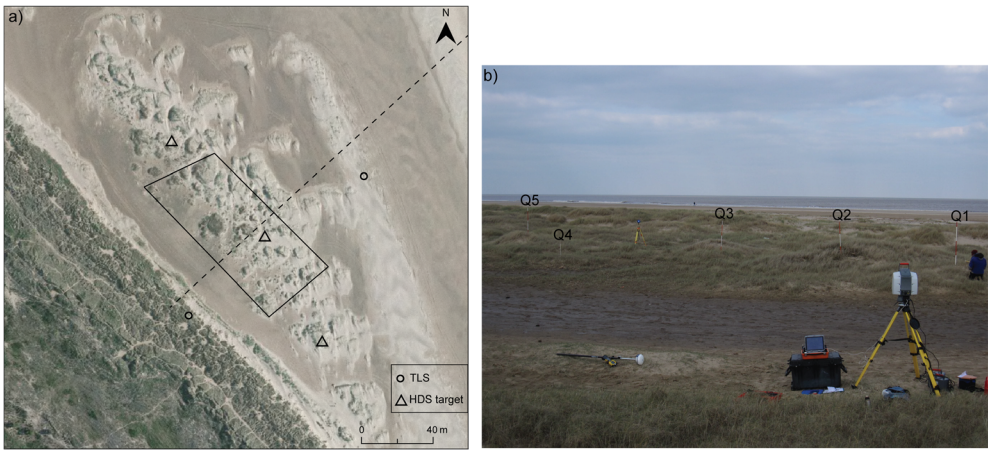

Figure 2. (a) 2010 aerial photograph of field site showing locations of terrestrial laser scanner and HDS targets. The dotted line indicates the location of the cross-shore profiles shown in Figure 4. (b) Ground photograph showing deployment of the terrestrial laser scanner from the landward foredunes and locations of the five test quadrats. This figure is available in colour online at wileyonlinelibrary.com/journal/espl

1.70 m above the ground. Within the survey zone, three tripod-mounted Leica high-definition surveying (HDS) targets were located in the north, centre, and south of the embryo dune field (Figure 2). Identifiable in both acquisitions, the HDS targets were used to acquire an accurate alignment of the survey scans. The locations of the HDS targets were measured using a real-time kinematic global positioning system (RTK-GPS) to enable accurate georeferencing (accuracies of ±10 mm horizontally and ±20 mm vertically) of the TLS survey into the British National Grid where the planimetric reference framework is OSGB36 and elevations are determined relative to mean sea level (ODN). Scan data were collected at 10 mm resolution and were corrected for atmospheric temperature and pressure which affect the speed of the propagated infrared signal. The quality of the individual point in a point cloud can also be influenced by scanner mechanism, scanned surface properties and scanning geometry (Soudarissanane *et al.*, 2011).

TLS data processing

Post-processing was done in three stages: (a) scan registration, (b) georeferencing and (c) digital elevation model (DEM) generation. The first two stages were performed using Cyclone software (Leica Geosystems), constructed to control the scanning procedures and to process and register point cloud data, potentially consisting of many millions of XYZ point coordinates. The scan registration involved a semi-automatic merging of the individual scan acquisitions into a single aligned local coordinate system initially. This TLS point cloud or mosaic was then georeferenced to the same external reference frame using the RTK-GPS validation HDS targets. The parameters for the reference frame transformation were determined by matching the coordinates of the three targets as measured by both the TLS and RTK-GPS. For each survey, the root mean square (RMS) residual error for three-dimensional similarity transformation was below 0.017 mm. Errors introduced during georeferencing can be caused by the inaccuracies of the RTK-GPS measurements, the centroiding algorithm used to determine the scanned control point coordinates, and also the inability of the Cyclone software to accommodate the local scale factor necessary to georeference the point cloud to the Ordnance Survey projection. For each survey, the final georeferenced TLS point cloud mosaic comprised an average of three million data points (x,y,z) at a sampling resolution of 10 mm. After georeferencing, the points from the HDS targets were manually removed. It was then possible to export the georeferenced point clouds to ArcView 9.3 software to generate continuous DEMs. Due to computer processing capacity it was not possible to examine the entire dune field in detail. Instead, a representative sub-section of the central dune field covering an area 90 m × 40 m and located on the upper beach was selected for detailed analysis. This reduced the size of the point clouds for DEM generation to an average of 1 860 000 points (Table I).

Estimation and corrections for vegetation derived error

The embryo dunes are vegetated in some areas and this can cause potential errors in measurements of topography if the TLS data point is returned from the vegetation rather than the underlying surface. The area of the vegetated embryo dunes could not be characterized from the images from the interior camera of the TLS due to over-exposure and poor quality. However, overall vegetation was determined from the aerial photographs in summer 2009, relevant to surveys in July 2009, October 2009 and January 2010, and in summer 2010 for more recent surveys. In 2009, 10.7% of the TLS survey zone comprised vegetated embryo dunes and 1.69% unvegetated embryo dunes with the remaining 87.6% of the area being non-dune areas (i.e. interdunes and upper beach). The areas of vegetated and unvegetated embryo dunes had expanded to 14.24% and 5.34%, respectively, of the TLS survey area by summer 2010, thus decreasing the non-dune area.

Potential elevation errors, and hence measurements of surface change of the dunes, due to the presence of vegetation were evaluated in two ways using a series of marked quadrats (1 m × 0.5 m) with different vegetation characteristics (Table II) and tested against manual field measurements of the vegetation. The field measurements of vegetation in the quadrats were undertaken using a standard point-intercept method (Floyd and Anderson, 1987) by deploying a 10-point sampling frame twice within each quadrat (i.e. 20-points per 1 m × 0.5 m area). All the quadrats were located on the landward side of the dunes. The tests of vegetation impact were undertaken in winter 2011, summer 2011 and winter 2012 (i.e. not concurrently with the main TLS surveys). For each quadrat, although there is some inter-seasonal variability, there were no statistically significant differences between vegetation height or percentage cover amongst the three surveys. Climatic conditions (temperature and rainfall) at the site for both the main TLS surveys and the vegetation tests were comparable; annual rainfall (mean daily maximum temperature) was 650 mm (13.31 °C), 642.25 mm (12.52 °C) and 696.50 mm (14.26 °C) in 2009, 2010 and 2011, respectively. This suggests that any

Table I. Summary of the seasonal (S) and vegetation test (VDE) TLS survey characteristics

Date	Scan resolution (m)	TLS registration error (m)	Number of data points in the point cloud used to generate DEM	RMS error of the DEM (m)	DEM accuracy: mean error and standard deviation (m)
S1: 1 July 2009 (Summer)	0.01	0.005	2 086 493	0.064	0.045 ± 0.059
S2: 8 October 2009 (Autumn)	0.01	0.017	1 868 126	0.066	0.042 ± 0.051
S3: 21 January 2010 (Winter)	0.01	0.014	1 618 598	0.064	0.039 ± 0.050
S4: 22 April 2010 (Spring)	0.01	0.005	1 789 912	0.057	0.035 ± 0.045
S5: 29 June 2010 (Summer)	0.01	0.004	1 799 522	0.067	0.047 ± 0.048
S6: 20 October 2010 (Autumn)	0.01	0.006	2 145 943	0.068	0.048 ± 0.049
VDE1: 22 February 2011	0.001	0.006			
VDE2: 5 July 2011	0.001	0.004			
VDE3: 19 March 2012	0.01	0.006			

Table II. Comparison of actual versus estimated vegetation characteristics

		Field vegetation measurements			Estimated vegetation height using survey data (m)			Difference.between TLS and GPS surface estimates (m)
Survey		Percentage cover	Maximum height (m)	Mean height (m)	$Zmax_{veg} - Zgps$	$Zmean_{veg} - Zgps$	$Zmax_{veg} - Zmin_{veg}$	$Zmin_{veg} - Zgps$
22 February 2011 (Method 1)	Q1	60	0.3	0.17	0.22	0.17	0.086	0.14
	Q2	70	0.25	0.18	0.22	0.09	0.181	0.04
	Q3	40	0.26	0.17	0.19	0.09	0.144	0.05
	Q4	48	0.16	0.07	0.17	0.10	0.117	0.06
	Q5	80	0.27	0.18	0.21	0.13	0.168	0.05
5 July 2011 (Method 1)	Q1	57	0.2	0.06	0.24	0.09	0.215	0.03
	Q2	97	0.39	0.25	0.34	0.29	0.238	0.10
	Q3	32	0.13	0.075	0.17	0.05	0.158	0.01
	Q4	51	0.15	0.07	0.25	0.13	0.211	0.04
	Q5	70	0.12	0.07	0.11	0.04	0.082	0.03
19 March 2012 (Method 2)					$Zmax_{veg} - Zmax_{noveg}$	$Zmean_{veg} - Zmean_{noveg}$		
	Q1	76	0.29	0.17	0.18	0.13		
	Q3	30	0.22	0.16	0.27	0.19		
	Q4	55	0.15	0.07	0.18	0.10		
	Q5	90	0.25	0.18	0.25	0.20		

conclusions from the 2011/2012 vegetation tests can be applied to the 2009/2010 surveys with reasonable confidence.

Method 1: In theory, it should be possible to evaluate the impact of vegetation on the TLS survey by comparing the TLS data with a survey of the dune surface. If vegetation, rather than the ground surface is being detected, the difference between the maximum (mean) TLS data point values for a given area and a surface survey should be related to the field measurements of maximum (mean) vegetation height. To test this, on 22 February 2011 and 5 July 2011 five quadrats were scanned at a resolution of 1 mm using the TLS (registration error 0.006 m for both surveys). On the same days a high resolution RTK-GPS ground survey was also undertaken within the quadrats with a point spacing of *c.* 0.05 m. Given that the topographic variability of the dune will affect the range of elevation in a given area, calculations for maximum (mean) values in the TLS point cloud were made using a moving window with a fixed size of 0.05 m (to correspond with the RTK-GPS survey). The maximum ($Zmax_{veg}$), minimum ($Zmin_{veg}$) and mean ($Zmean_{veg}$) of the TLS elevation point cloud within each 0.05 m window was determined. The estimated maximum (mean) vegetation height is therefore calculated by $Zmax_{veg}$ – Zgps ($Zmean_{veg}$ – Zgps) for the same window. An additional possibility is that the minimum value of the TLS point cloud data within each square could adequately represent the topographic surface if the laser can penetrate the vegetation (Coveney and Fotheringham, 2011). This was tested by comparing the minimum TLS value ($Zmin_{veg}$) against Zgps. Finally, if $Zmin_{veg}$ adequately represents the surface and $Zmax_{veg}$ is detecting the top of the vegetation canopy, then the difference between the two ($Zmax_{veg}$ – $Zmin_{veg}$) should correlate with field measurements of maximum vegetation height.

Method 2: In March 2012 a second test was carried out using four of the same quadrats (quadrat 2 was not surveyed due to battery failure). A TLS survey was carried out at a resolution of 0.01 m on the vegetated quadrats. The above-ground vegetation within the quadrats (and a border *c.* 0.3 m wide around the quadrat) was then removed to ground level using shears and the TLS surveys repeated. As mentioned earlier, the estimated maximum (mean) vegetation height is calculated by $Zmax_{veg}$ – $Zmax_{noveg}$ ($Zmean_{veg}$ – $Zmean_{noveg}$) for a 0.05 m grid.

Figure 3 shows the relationship between measured and estimated vegetation and elevation using Method 1. For maximum vegetation height there is a statistically significant relationship between the estimates ($Zmax_{veg}$ – Zgps) and field measurements ($R^2 = 0.79$, $p < 0.05$); the relationship is less strong, but still significant, for estimates of mean vegetation height ($R^2 = 0.64$, $p < 0.05$). The average of maximum and mean estimated residuals was 0.036 m and 0.038 m, respectively. Figure 3c shows the relationship between $Zmin_{veg}$ and Zgps which is positive and significant ($R^2 = 0.92$, $p < 0.05$). The mean difference between the two values is 0.051 m. For all the earlier relationships the greatest errors are associated with quadrats with dense vegetation cover. For example $Zmin_{veg}$ – Zgps ranges from 0.011 m for Quadrat 3 which has a vegetation cover of 32% (5 July 2011) to 0.136 m for Quadrat 1 with a vegetation cover of 60% (22 February 2011). Overall the error increases with increasing vegetation cover, which likely reflects reduced laser penetration with more dense cover, however there are no significant relationships between $Zmax_{veg}$, $Zmean_{veg}$ and percentage vegetation cover. Finally, the difference between estimates of maximum vegetation height from the TLS data alone ($Zmax_{veg}$ – $Zmin_{veg}$) and field measurements of vegetation height is relatively small (0.084 m), suggesting there may be some potential for using TLS data for vegetation height characterization. Confirmation of this potential is provided by the results of Method 2 in which the average maximum vegetation height estimated using $Zmax_{veg}$ – $Zmax_{noveg}$ is 0.22 m compared with 0.228 m from the field surveys, and the mean vegetation height is 0.155 m ($Zmean_{veg}$ – $Zmean_{noveg}$) compared with 0.145 m (Table II). Clearly, this second method is not a practical way to determine survey errors associated with vegetation across large areas given that it is destructive.

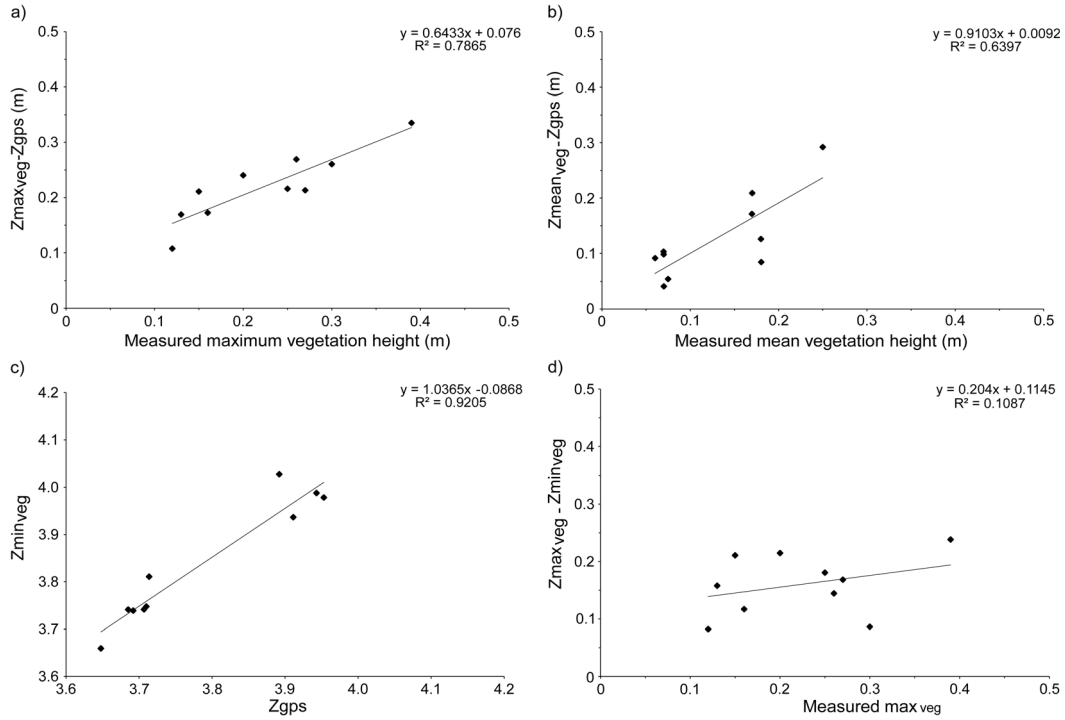

Figure 3. Results of tests to determine the relationships between (a) measured maximum vegetation height and $Zmax_{veg}$ – Zgps; (b) measured mean vegetation height and $Zmean_{veg}$ – Zgps; (c) Zgps and $Zmin_{veg}$; (d) measured maximum vegetation height and $Zmax_{veg}$ – $Zmin_{veg}$. See text for details.

The results of the vegetation tests and relationships shown in Figure 3 indicate that from the TLS point cloud data, the best representation of topographic surface elevation will be given by the minimum values within each sample window. These data were therefore used to construct DEMs for each of the seasonal surveys.

DEM generation

For each seasonal survey, a DEM was generated from the minimum values in the point clouds within a cell size of 0.05 m and then re-sampled to 0.5 m grid spacing using Inverse Distance Weighted interpolation, set to a power of two with the radius limited to the closest 12 points in order to negate both distant points whilst honouring nearest neighbours. This approach has been demonstrated as effective for terrain modelling with a large topographical variation (Burrough and McDonnell, 1998) so is appropriate for the site. Difference DEMs were produced to compare successive surveys in order to visualize the morphological changes, identify areas of deposition, erosion or no change within the embryo dune field and calculate the dune sand budgets related to ODN. For each survey, the RMS errors calculated between the seasonal interpolated DEM and survey point clouds ranged from 0.057 to 0.068 m (Table I). Accuracy assessments of the DEMs were also based upon the mean error and standard deviation, which provide data to describe systematic and random effects respectively (Li, 1988; Chandler *et al.*, 2005). In all cases, both measures were below ±0.06 m (Table I). Quantifying the volume of sediment within coastal system components (such as beach, dunes, cliffs) can be useful for understanding sediment budgets and interactions amongst landforms (e.g. Saye *et al.*, 2005; Young and Asford, 2006). The monthly rate of change in the volume of sand (Rvs; in $m^3\ m^{-2}\,month^{-1}$) within the DEM area was calculated by dividing the total volume of change (Vs; in m^3) by the area of the scan survey (A; in m^2) and the time between surveys (T; in months) following the method of Young and Asford (2006) such that $Rvs = Vs/(A \times T)$.

Short-term process experiments

To gain some understanding of the processes forming and maintaining the embryo dunes, a series of simple, one-day monitoring experiments was conducted within a few days of each of the TLS surveys to characterize airflow at the site (summarized in Table III). For each experiment, seven monitoring sites were established in a cross-shore transect. Site locations are shown in Figure 4 and described in Table IV. It was not possible to use a site within the embryo dunes themselves, however measurements were made at the seaward foot of the dunes and on the upper beach which give an indication of airflow and sediment transport upwind and downwind of the embryo dune system. A standard methodology was adopted using differential fractional speed-up ratios to determine spatial patterns of airflow from asynchronous data sets normalized to a continually recording reference station (e.g. Wiggs *et al.*, 2002; Hesp *et al.*, 2005; Bullard and Austin, 2011). A reference station to monitor wind speed and direction was established and located on the secondary foredune crest in October 2009 and on the middle beach for all other experiments. This comprised Vector A-100R pulse-count rotating cup anemometers in a vertical array at heights of 0.22 m, 0.5 m, 0.8 m, 1.2 m and 1.7 m, a Vector W-200P wind vane at 0.5 m and a R.M.Young 5013 combined wind speed and direction sensor at 2.4 m. It also included a Sensit H11B saltation impact sensor and a thermistor at ground level. Surface moisture content was measured using a calibrated hand-held Thetaprobe ML2x every two hours. A mobile monitoring array with the same instrumentation as the reference station was deployed simultaneously at each site for periods of at least 20 minutes. At each site wind speed was integrated over 10 second intervals for periods of one minute. Velocity data from the two measurement arrays was used to calculate the fractional speed-up ratio (δs) as defined by Jackson and Hunt (1975):

$$\delta s = U_{\mathrm{mob}} z / U_{\mathrm{ref}} z$$

where $U_{\mathrm{mob}}z$ is the wind speed at height z on the mobile measurement array, and $U_{\mathrm{ref}}z$ is the wind speed at height z on the reference array. The speed-up ratio allows an assessment of the changes in relative wind speed at each location, where $\delta s > 1$ indicates acceleration in velocity compared to the reference station at the same height and a value of < 1 indicates deceleration. It can be used for all winds (above or below threshold) to indicate changes in potential sediment transport between sites such that a downwind increase in δs suggests increasing potential sediment transport (i.e. entrainment) whereas a downwind decrease suggests decreasing potential transport (i.e. deposition).

The horizontal flux of wind-blown material was measured using vertical arrays of Fryrear traps (Fryrear, 1986) modified to include a rainhood (Shao *et al.*, 1993) and mounted at heights of 0.22 m, 0.5 m, 0.8 m and 1.2 m. Provided wind direction remained constant during the day, these were emptied at the end of the total daily measurement period and the weight of trapped sand converted to a rate of transport in $g\ m^{-1}\ h^{-1}$. Although in several instances sediment was trapped in the Fryrear traps, very little data was recorded by the saltation impact sensors and the results are not presented here. The most likely reason is that the combination of light winds and fine sediments meant particle impacts were not recorded (Stout and Zobeck, 1996; Bullard and Austin, 2011).

Table III. Summary of conditions at the reference station during the short-term process experiments

Date	Mean wind speed at 2.4 m	Wind direction			Mean air temperature (°C)
	In $m\ s^{-1}$	In degrees	Description	Incident angle relative to foredune crest	
15 October 2009	1.10 – below threshold (±0.3)	118 (±9)	Oblique onshore	24	15
27 January 2010	6.30 (±0.6)	280 (±3)	Oblique offshore	30	6
29 April 2010	2.18 – below threshold (±0.6)	290 (±5)	Oblique offshore	40	20
8 July 2010	4.11 (±0.8)	242 (±12)	Direct offshore	12	26

Note: Standard deviations of the records are in brackets.

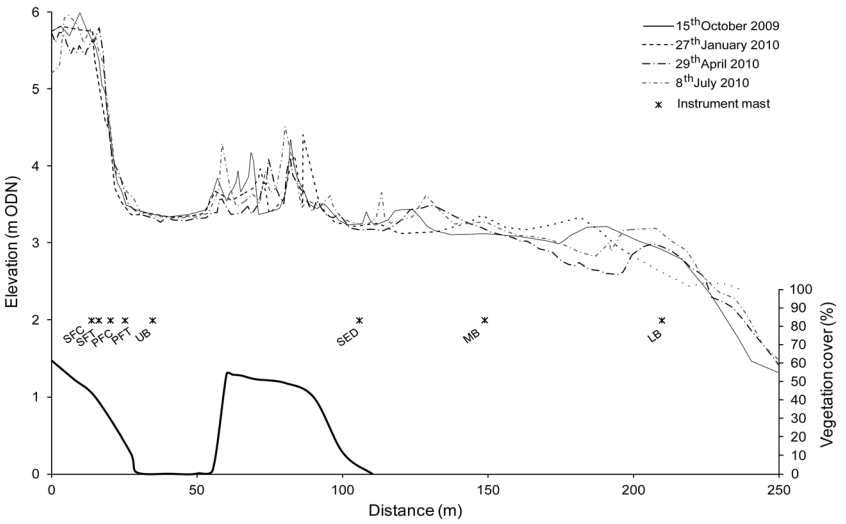

Figure 4. Seasonal cross-shore topographic profiles along which instruments were located for the short-term process experiments. Vegetation density along the transect is also shown in solid line

Table IV. Geomorphology and sedimentology of sampling sites used for the short-term process experiments

Site	Geomorphology	Sedimentology (μm)			
		Range of D_{50}	D_{50}	Mode	σ
SFC	Secondary foredune crest	248–272	255	201	1.03
SFT	Secondary foredune toe	251–270	259	206	1.03
PFC	Primary foredune crest	246–262	257	259	1.28
PFT	Primary foredune toe – junction between the primary foredune and the beach face, approximately at HAT	246–266	255	251	1.32
UB	Upper beach – upper section of tidal beach between $z = 3.5$ m and MHWS	238–242	240	245	1.28
SED	Seaward of the embryo dunes	253–261	258	258	1.28
MB	Middle beach – seaward of the embryo dunes	241–251	257	245	1.27
LB	Lower beach between $z = 3$ m and MHW	253–269	260	261	1.3

Note: MHWS, mean high water spring; MHW, mean high water.

Meteorological data and water level analysis

The development and persistence of the embryo dunes depends, amongst other things, on the balance between sediment input by constructive sand transporting winds and the magnitude and frequency of high energy marine erosion events such as storm surges. Hourly mean wind speed and direction (10° sectors) measured at the nearest long-term meteorological station, Donna Nook (12 km north of Theddlethorpe) (Figure 1), were obtained from the British Meteorological Data Centre for the period from 1 August 2000 to 31 July 2011. At Donna Nook, the meteorological instruments are mounted at a height of 8 m above the ground surface and all the land between the site at Theddlethorpe and Donna Nook is less than 5 m above ODN. These data are therefore assumed to be representative of meteorological conditions at the study site. For sediments at Theddlethorpe, Bagnold's (1941) critical threshold equation suggests a fluid critical shear velocity of 0.23 m s^{-1}. Using this value, and an approximate value for surface roughness (z_0) of D_{50}/30, the Karman–Prandtl velocity distribution indicates that sand transport should occur when wind speeds of 7.8 m s^{-1} are recorded at 8 m height (i.e. at Donna Nook). The short-term process studies conducted for this paper indicate sand transport occurred at the seaward side of the embryo dunes with a mean wind speed of 4.11 m s^{-1} at 2.4 m height and with high surface gravimetric moisture contents of 25 to 30%, but the field threshold value is unknown. The 4.11 m s^{-1} would translate to a wind speed of 12 m s^{-1} at 8 m height, but is likely to be an over-estimate of the wind speed at which potential sand transport could occur under drier conditions. Field experiments over the foredune at Mablethorpe, located 1 km south of the study site recorded sand transport during winds of 3.1 m s^{-1} at 2.4 m height with *c.* 10% surface moisture (Montreuil, 2012) which corresponds to a wind speed of *c.* 9.1 m s^{-1} at 8 m height. Given these three estimates, a value of 8 m s^{-1} at Donna Nook was taken to indicate the minimum velocity for potential sand transporting winds at Theddlethorpe. The occurrence of onshore (0° to < 150°), alongshore (150°–170°, 330°–350°) and offshore (> 170° to 330°) winds ≥ 8 m s^{-1} (i.e. potential sand transporting winds) was used to determine their relative magnitude and frequency for the year prior to each aerial photograph survey. This was taken as from August in the year preceding the survey photograph acquisition. The frequency of potential sand transporting winds was also assessed on a seasonal basis from 1 July 2009 to 20 October 2010 corresponding to the seasonal TLS scans.

Marine forcing factor analysis focused on high energy events, which determine the periods of time when the embryo dune could be reached by potentially erosive high tides. Storm surge is one of the most likely drivers of significant sediment transport and morphological change. Fifteen minute measurements of water level at Immingham (north of Theddlethorpe – Figure 1) were supplied by the British Oceanographic Data Centre (BODC). Data relating to water levels obtained in Chart Datum were converted to ODN using the conversions for Skegness given by BODC (http://www.bodc.ac.uk). To identify the potential eroding events, the frequency of storm surges occurring between successive seasonal surveys was determined.

A storm surge event was defined as the occurrence of onshore and/or landward directed alongshore (340°–160°) winds $\geq 10\,m\,s^{-1}$ concurrent with a water level ≥ 3.5 m ODN, which corresponds to the maximum elevation of the landward side of the embryo dune field. The duration of each storm surge event identified is determined by the period of time these two conditions coincided and is given in Table V.

Results

Decadal development of the embryo dune field

The field of embryo dunes was not visible on aerial photographs taken in summer 2000 (Figure 1) but by the following summer a small area of dunes 13.11 m^2 in size could be seen. The area of dunes expanded steadily from 2002 to 2006 by which time it covered 568.75 m^2 (Figure 5). The size of the dune field expanded rapidly between 2006 and 2007, more than doubling in size from 568.75 m^2 to 1201.75 m^2. The LiDAR data indicate an increase in sand volume above ODN of 2444.8 m^3 from 70 797.45 m^3 in 2001 to 73 242.25 m^3 in 2007 across the whole dune field and beach. Specifically, the sand gain of the embryo dunes was 2018.86 m^3 corresponding to a vertical gain of 1.68 m (0.28 m yr^{-1}) from 2001 to 2007. The dune field reduced in areal extent in 2008 before continuing to expand in all years to 2011 by which time it covered over 3605.9 m^2. Figure 5 also shows the mean, minimum and maximum distance between the established foredune toe (HAT) and the landward side of the embryo dunes. From 2001 to 2004 not all of the five transects crossed the embryo dune field because it only covered a small area; the maximum distance therefore reflects distance from the foredunes to the landward intertidal bar (i.e. mean high water, MHW). From 2005 to 2011 all five transects crossed both the foredune and the embryo dunes and the average gap between the two gradually decreased from 55.48 m in 2005 to 26.06 m in 2011.

Between 1 August 2000 and 31 July 2011, wind velocities were typically below $8\,m\,s^{-1}$ (> 70% of the time). With the exception of s2002–s2003 and s2009 and s2010, sand-transporting winds ($\geq 8\,m\,s^{-1}$) were more frequently directed offshore than onshore. The frequency of offshore winds ($\geq 8\,m\,s^{-1}$) ranged from 8.36% in s2009–s2010 to 17.99% in s2001–s2002 compared with onshore winds which occurred for just 6.76% of the time in s2001–s2002 but nearly 12% of the time in the following year (Table V). The mean wind speed of onshore winds $\geq 8\,m\,s^{-1}$ was temporally consistent and in the range 10.38–10.99 $m\,s^{-1}$ throughout the decade. Offshore sand-transporting winds were also consistent but had a slightly lower mean velocity (9.78–10.69 $m\,s^{-1}$). Potential sand transporting alongshore winds occurred less than 5.3% of the time. Wind climate conditions were thus consistent from year to year. The highest winds were generally recorded in autumn–winter seasons.

As defined here, storm surges are fairly infrequent along this coastline and typically of short duration (< 2 hours). Three and four storm surges characterized by wind speed $\geq 10\,m\,s^{-1}$ and water level reaching ≥ 3.5 m occurred over the period s2000–s2001 and s2001–s2002, respectively. However only one storm surge was recorded in s2003–s2004. Five storm surge events were recorded in s2003–s2004 and three events in s2004–s2005, while only one took place in s2005–s2006. The frequency of storm surge was relatively high in s2006–s2007 and s2007–s2008 with 10 and four events recorded, respectively. Only one and three storm surges, each of relatively low duration, occurred in s2008–s2009 and s2009–s2010,

Table V. Summary of the potential sand transporting winds ($\geq 8\,m\,s^{-1}$) and water level conditions between summer (s) 2000 and summer 2011

Year	Efficient onshore winds		Efficient offshore winds		Efficient alongshore winds		Storm surge	
	Frequency (%)	Mean velocity ($m\,s^{-1}$)	Frequency (%)	Mean velocity ($m\,s^{-1}$)	Frequency (%)	Mean velocity ($m\,s^{-1}$)	Number	Average duration (h)
s2000–s2001	9.69	10.77	11.98	10.20	5.28	11.02	3	0.42
s2001–s2002	6.76	10.46	17.99	10.55	3.72	11.16	4	1.31
s2002–s2003	11.96	10.81	10.29	9.78	3.85	10.62	1	1
s2003–s2004	9.73	10.54	11.80	10.28	3.80	10.36	5	0.9
s2004–s2005	9.81	10.43	14.05	10.41	3.17	11.23	3	1.75
s2005–s2006	8.65	10.44	10.77	10.16	3.62	10.31	1	1
s2006–s2007	7.22	10.38	14.86	10.69	4.32	11.00	10	1.45
s2007–s2008	7.83	10.99	15.66	10.41	4.95	11.56	4	1
s2008–s2009	10.77	10.42	11.29	10.14	2.70	10.76	1	0.75
s2009–s2010	10.06	10.82	8.36	10.30	4.19	10.93	3	0.67
s2010–s2011	8.87	10.76	11.12	10.25	4.12	10.55	3	0.92

Note: Storm surge is defined as an event when onshore/landward directed alongshore winds $\geq 10\,m\,s^{-1}$ and water levels ≥ 3 m coincide.

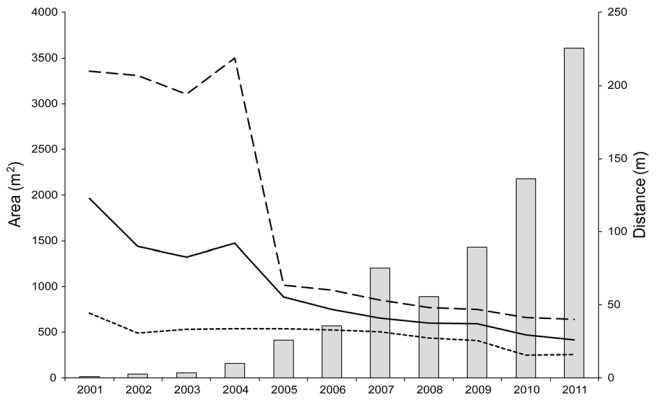

Figure 5. Annual changes in the area of the field of embryo dunes and distance between foredunes and landward of the embryo dunes from 2001 to 2011. The dashed, solid and dotted lines correspond to the maximum, mean and minimum distances, respectively

respectively. Despite these storm surges, the only sign of erosion in the aerial photographs was the change in aerial footprint, with no other signs such as scarping. This may in part be due to the timing of aerial photograph acquisition, which is during the summer when dune recovery is more likely to take place.

Seasonal morphological changes and forcing factors

The overall topographic data (corrected to account for vegetation cover) for the seasonal TLS surveys of a 90 m × 40 m sub-section of the embryo dune field are summarized in Figures 6 and 7. The embryo dunes experienced a net sand gain of 150.92 m^3 above ODN over the 16-month monitoring period, however patterns of erosion and accretion were both spatially and temporally variable. The area of unvegetated beach within the TLS survey was flat and relatively stable over the monitoring period, so that any overall volume changes were primarily due to dune development rather than beach accretion or erosion (which is typically ≤ ±0.1 m for each survey).

In summer 2009 (July), the DEM shows three major embryo dunes up to *c.* 4.8 m ODN located in the north and centre of the area (Figure 6). The south is dominated by small, clustered sand hummocks, while the landward side is relatively flat and level at a height of *c.* 3.2 m ODN. Between July and October 2009, the volume of sand within the dunes increased slightly by 30.32 m^3. The difference DEM generally indicates little overall change, however a few limited spots underwent sand deposition (0.1 m to 0.82 m vertical change). The main embryo dunes located in the centre-landward part of the survey and also to the south-seaward side were reduced in height with an average vertical erosion of 0.69 m and 0.91 m, respectively, despite the relatively low frequency of sand transporting winds (Table VI). Potential sand transporting offshore winds (≥ 8 m s^{-1}) blew 8.74 % of the time with a mean speed of nearly 9.6 m s^{-1}. Onshore and alongshore winds above 8 m s^{-1} only occurred 4.1% and 1.4 % of the time, respectively. There were no high water level events during this monitoring period.

From October 2009 to January 2010 (autumn–winter), the dunes experienced substantial sand losses of 315.49 m^3 corresponding to a net sand budget change of –90.14 m^3 $month^{-1}$ and a volumetric rate of change of –0.026 m^3 m^{-2} $month^{-1}$ across the whole TLS survey area. The spatial footprint of the

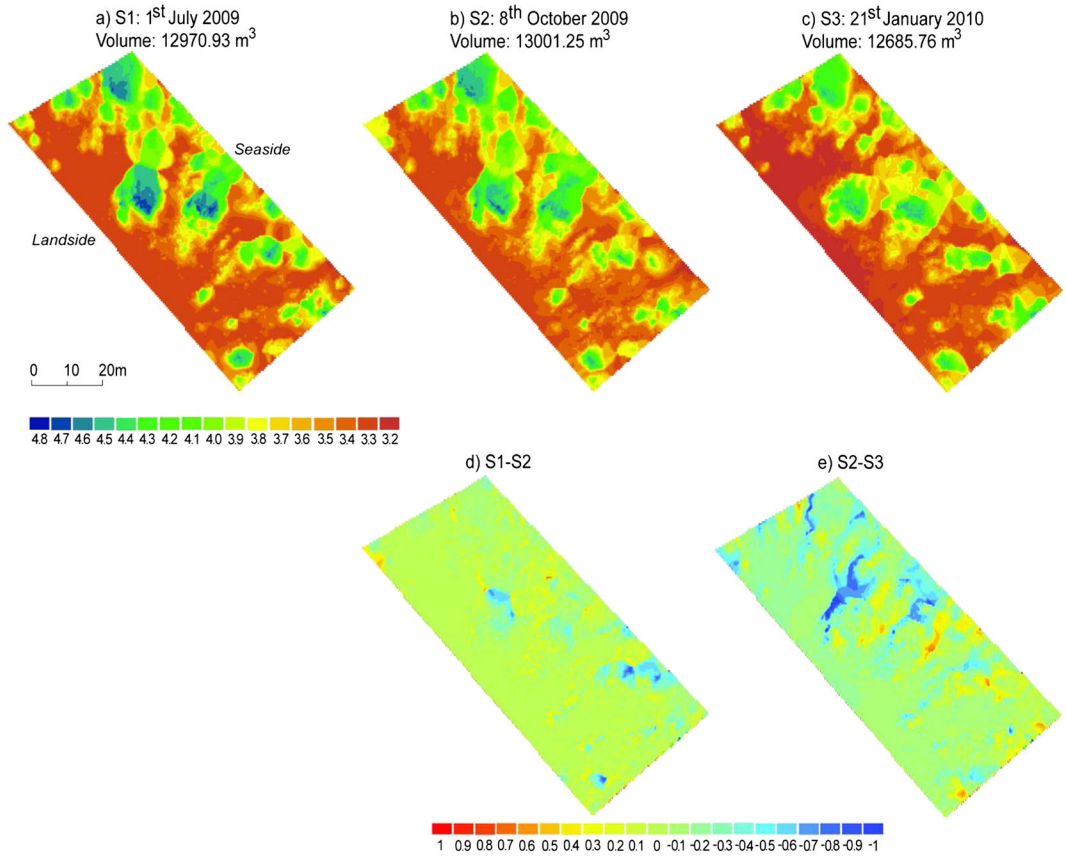

Figure 6. Digital elevation models for (a) S1 July 2009, (b) S2 October 2009, (c) S3 January 2010; and DEMs of difference to highlight topographic changes between (d) S1 and S2, (e) S2 and S3. This figure is available in colour online at wileyonlinelibrary.com/journal/espl

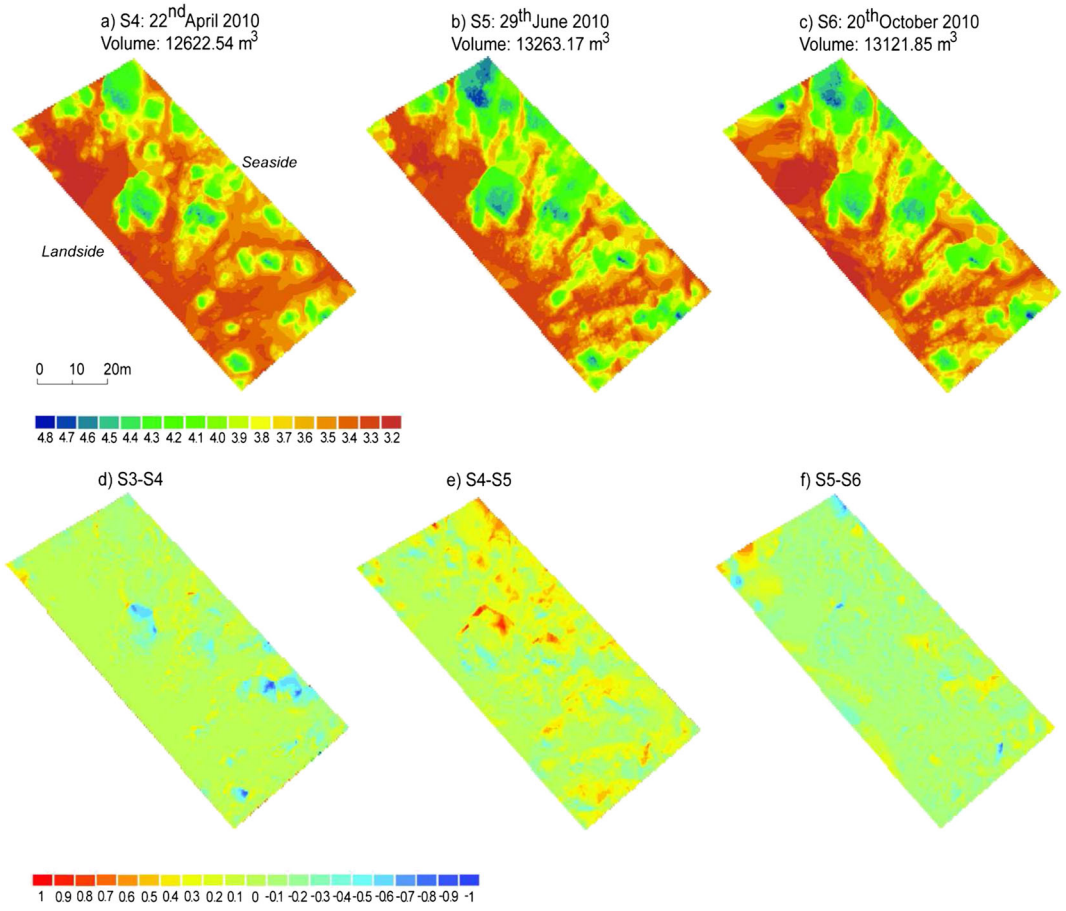

Figure 7. Digital elevation models for (a) S4 April 2010, (b) S5 June 2010, (c) S6 October 2010; and DEMs of difference to highlight topographic changes between (d) S3 and S4, (e) S4 and S5, (f) S5 and S6. This figure is available in colour online at wileyonlinelibrary.com/journal/espl

embryo dune field was slightly modified but the difference DEM clearly shows the development of one corridor through the dunes at the north-seaward side and two others between the main embryo dunes in the centre, which are oriented northeast and which have a length of *c.* 25 m and 17 m. These corridors are caused by erosion of the dunes by, on average, 0.7 m along the corridor lengths. During this winter period, strong winds were recorded up to 19 m s^{-1} (Table VI). The most frequent potential sand transporting winds were onshore (14%), followed by offshore winds which occurred 12.66% of the time. Two storm surges with winds $\geq$ 10 m s^{-1} and water level $\geq$ 3.5 m occurred, both at the end of October 2009.

For the survey in April 2010, a sand loss of 63.22 m^3 was recorded within the embryo dune field (Figure 7). The difference DEM shows that the erosion was mainly localized towards the south-seaward side and the centre of the main embryo dune field, contrasting with positive morphological changes on the landward side and in the northeast part of the survey area. From April to the end of June 2010, the embryo dune field underwent accretion at the seaward side while the landward side remained relatively unchanged. Sand gain across the whole area exceeded 640.63 m^3, corresponding to a volumetric rate of change of 0.08 m^3 m^{-2} month^{-1}. During the surveys in April and July 2010, onshore winds above 8 m s^{-1} prevailed with a frequency of 10.6%, while the frequencies of potential sand transporting offshore and alongshore winds were relatively low (Table VI). No storm surges were recorded during this summer period.

The autumn survey in October 2010 shows that the three major embryo dunes were still present, but had become larger and slightly lower than when first surveyed in July 2009. The northern main embryo dunes have started to merge with a smaller dune and the seaward side embryo dunes have generally expanded in area. The embryo dune field lost 141.32 m^3 of sand (equivalent to 0.01 m^3 m^{-2} month^{-1}) between the end of June and October 2010. During this monitoring period onshore, offshore and alongshore strong winds ($\geq$ 8 m s^{-1}) accounted for 6.93%, 8.12% and 5.66%, respectively, so that potential sand transporting offshore winds slightly dominated (Table VI). Storm surges occurred three times during this period. The first storm surge event occurred at the end of August and the most significant storm surge event occurred on 24 September 2010. During this event, wind blew from north (350°) with a mean speed up to 15 m s^{-1} and induced a surge 0.39 m high.

Airflow and sediment transport over the embryo dunes

Figure 4 shows the cross-shore topographic profiles along which the instruments were located for the short-term process experiments. As with the DEMs, the profiles show seasonal changes in embryo dune morphology, confirming that the dunes were taller during the summer months than the winter months. The profile also highlights the development of small ephemeral dunes that formed seawards of the main embryo dune field (*c.* 120–140 m along the transect). For example dunes were present in this area in October 2009 but disappeared before the January 2010 profile was measured. Landwards of the main embryo dune field the base of the foredune was slightly narrower during the winter months compared with the summer months but there was no

Table VI. Summary of seasonal analysis of wind and marine conditions and volume changes recorded in the DEM

	Efficient onshore winds			Efficient offshore winds			Efficient alongshore winds			Water level	Sediment
		Velocity m s^{-1}			Velocity in m s^{-1}			Velocity in m s^{-1}		Events	Volume
	Frequency (%)	Mean	Maximum	Frequency (%)	Mean	Maximum	Frequency (%)	Mean	Maximum	≥3.5 m	change (m^3)
1 July–8 October 2009	4.06	9.61	12.86	8.74	9.57	14.92	1.38	9.52	11.83	0	30.32
8 October 2009–21 January 2010	14.03	11.66	19.55	12.66	10.84	18.04	5.20	10.95	16.46	2	–315.49
21 January–22 April 2010	9.28	9.88	14.4	7.90	9.73	13.89	3.31	9.52	14.4	1	–63.22
22 April–29 June 2010	10.58	9.98	14.92	1.88	11.4	14.92	6.23	11.97	11.97	0	640.63
29 June–20 October 2010	6.93	10.27	15.95	8.12	10.23	16.98	5.66	11.38	18.52	3	–141.32

Note: Potential sand transporting winds correspond to winds ≥ 8 m s^{-1}.

systematic change in dune height. Seaward of the embryo dunes on the middle and lower beach the position of the intertidal bars changed seasonally. The most prominent bar was more landward in January 2010 than in October 2009, but in April and July 2010 it was further offshore.

Figure 8 summarizes the results of the short-term process experiments. Unfortunately no direct onshore winds were observed, however oblique onshore winds were recorded on 15 October 2009. On this date, the reference station was located on the secondary foredune crest which has a dense (60%) but low vegetation cover. Wind velocity on the middle beach was higher than at the reference station ($\delta s = 1.1$ at 0.22 m) but slowed at the seaward foot of the embryo dunes at all measurement heights ($\delta s = 0.77$ at 0.22 m) (Figure 8, left hand graphs). On the upper beach, landward of the embryo dunes, the shape of the velocity profile is very similar to that on the middle beach and winds speeds recovered to slightly higher than the reference station. Near-surface wind speed decreases substantially as the airflow reaches the primary foredune toe. Due to low wind speeds (Table III) no sediment transport was recorded at any point along the transect; high moisture levels were recorded on the beach (> 25%) but within the foredune surface moisture was typically 5% (Figure 8, right hand graphs).

Strong, direct offshore winds occurred during the experiment on 8 July 2010. The reference station was located on the middle beach and wind velocities at other cross-shore locations were lower than the reference values. On the foredune, near-surface airflow was slowest on the secondary foredune crest and gradually increased as it travelled over the primary foredunes (Figure 8). Wind directional variability was also low in all sub-units. This likely reflects a combination of flow recovery on the downwind side of the dunes and decreasing vegetation cover with increasing proximity to the beach. No sediment was trapped on the secondary foredune crest, however a small amount was trapped on the secondary foredune toe. On the primary foredune toe no near surface sediment transport was recorded, however 5 g m^{-1} h^{-1} was trapped at a height of 1.2 m. Wind speed continued to increase on the upper beach where *c.* 10 g m^{-1} h^{-1} of sediment was trapped at ≤ 0.8 m. Although some of this sediment may have been derived from the beach, the moisture content on the upper beach was 20%, which is likely to limit local entrainment, and the sediment is more likely to have been eroded from the foredunes. Wind speeds were higher on the seaward side of the embryo dunes than on the upper beach, but no sediment transport was recorded. This suggests that the sand being transported across the upper beach was trapped by vegetation on the embryo dunes and deposited.

Oblique offshore winds are common on the Lincolnshire coast (37%) and occurred during the experiments on 27 January and 29 April 2010, although wind speeds were relatively low during the spring (< 2.5 m s^{-1} at 2.4 m). As with direct offshore winds, near surface airflow accelerates as it passes over the primary foredune, upper beach and to the seaward side of the embryo dunes (Figure 8). Reduction in wind speed at the secondary foredune crest is most likely due to vegetation cover. For both experiments, wind directional variability was high over the foredunes (difference of 36° at 0.5 m high at the secondary foredune toe site compared to the reference mast on the middle beach). However, the wind direction stabilized over the beach whereas under highly oblique offshore winds, the wind direction remained variable on the upper beach and on the seaward side of the embryo dunes probably due to low wind speed. High moisture levels (January 2010) and low wind speeds (April 2010) mean that very little sediment transport was recorded during these

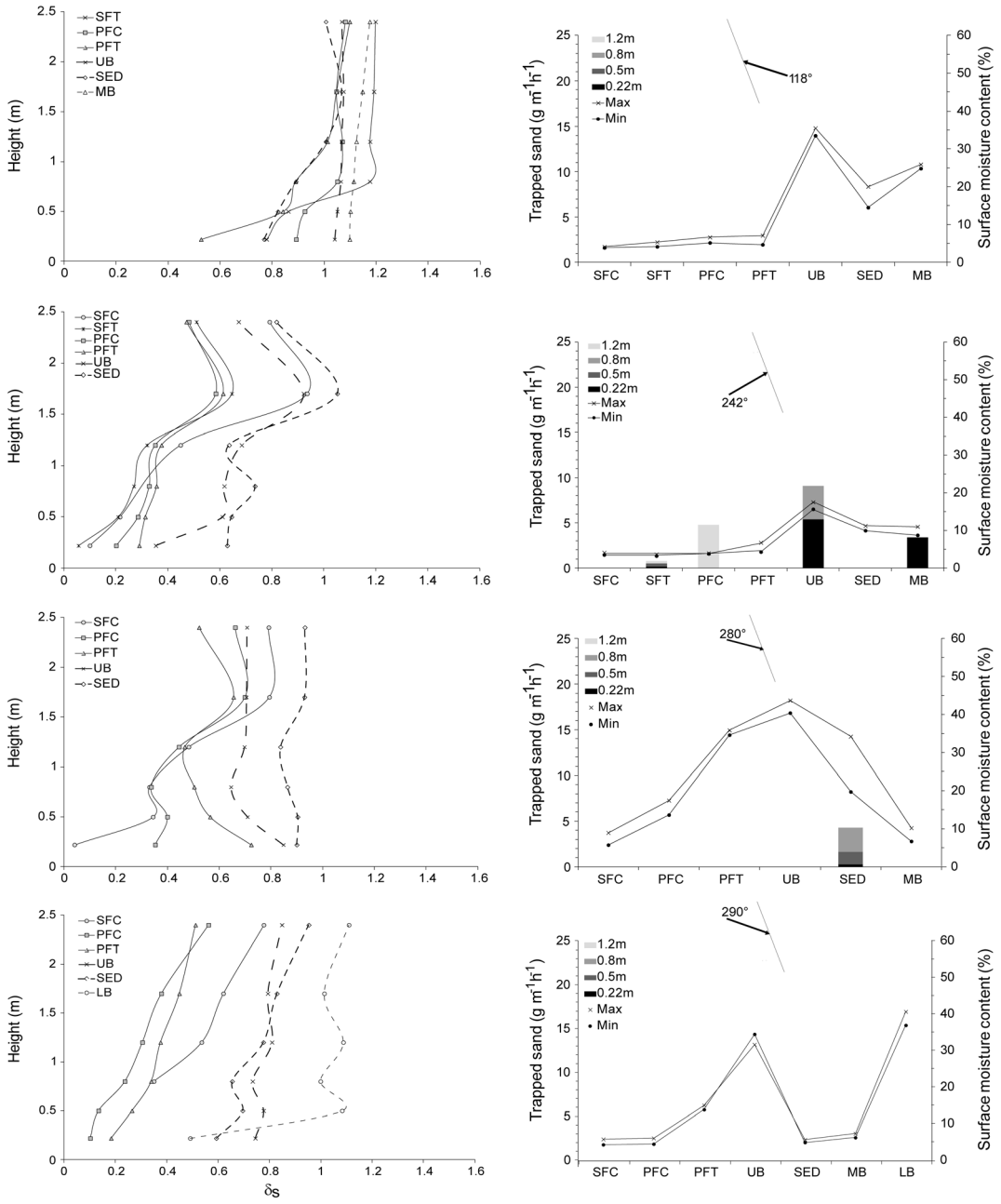

Figure 8. Summary of short-term experiments conducted from top to bottom on 15 October 2009, 8 July 2010, 29 April 2010, 27 January 2010. Left hand graphs: time-averaged fractional speed-up velocity profiles for different locations on the cross-shore profile (see Table IV for abbreviations). Right hand graphs: quantity of sand trapped at each location, and gravimetric moisture content along transect. Inset graph shows relative orientations of coastline and wind direction during the experiment.

experiments. However in January 2010 nearly $5\,g\,m^{-1}\,h^{-1}$ of sediment was trapped on the seaward side of the embryo dunes suggesting that material was being eroded from the dunes by the wind.

Discussion

Detection of topographic change using TLS on vegetated dunes

In this study we used TLS data to monitor seasonal changes in the topography of vegetated coastal dunes. The comparison of z values in the TLS point cloud (within a 0.05 m grid) above the differential global positioning system (DGPS)-derived surface indicates that at the study site, the maximum z values of the TLS laser returns provide a good representation of the maximum height of the vegetation, particularly where vegetation cover is dense. Where vegetation percentage cover is lower, the laser is returned from vegetation at a range of heights and may also be reflected from the ground surface which makes it harder to determine the vegetation characteristics (Wang *et al*., 2009). However, the minimum TLS value ($Zmin_{veg}$) compares well with the ground survey and, for nine of out 10 quadrats, the differences between values of $Zmin_{veg}$ and Zgps are ≤ 0.1 m. Values of $Zmin_{veg}$ are therefore assumed to provide a suitable representation of the ground surface and used to determine the DEMs of the site. Other studies have also suggested that minimum TLS values can provide a reasonable approximation of surface morphology. For example Guarnieri *et al*. (2009) and Schmid *et al*. (2011) successfully applied a similar technique to coastal salt marshes. Vegetation composition and density at a site will determine the overall utility of this filtering-type approach which is likely

to be less reliable in areas with multi-layered canopies and very dense vegetation (e.g. Rosso *et al.*, 2006).

Where TLS surveys are conducted once, such as to determine spatial variability only, both methods of determining vegetation-derived error tested here could be applied. However where temporal change in topography is of interest it is important to determine not only morphological changes but also possible impacts on the DEM of variation in vegetation characteristics such as cover, density and height. A short sequence of vegetation surveys within the embryo dune field showed no significant seasonal variation in vegetation cover or height. This may be because the surveyed central section of the dune field has developed over 10 years and the vegetation structure (species, percentage cover) on the dunes is no longer undergoing rapid change. Surveys by Natural England as well as the data presented here indicate the vegetation on the dunes is currently reasonably stable in terms of composition. Consequently the vegetation-derived error is likely to be similar for multiple surveys through time. The area surveyed seasonally using the TLS comprises both non-dunes (unvegetated interdunes and beach) and dunes; vegetated dunes are more extensive than unvegetated dunes. On the unvegetated beach the topographic differences between one seasonal survey and the next are typically $\leq \pm 0.1$ m. In contrast, the topographic changes detected, using the corrected DEMs, within the vegetated dunes are often substantial, with vertical erosion or deposition of $\geq \pm 0.5$ m being common; such a large change is greater than could be attributed to the combined errors of the TLS survey and the impact of vegetation. Vegetation cover plays an important role in the accretion of embryo dunes by trapping wind-blown sand and growing up through the deposits (Hesp, 1983, 1989; Arens, 1996). If the DEM were to be corrected for vegetation cover using a single estimate of vegetation height (e.g. $Zmax_{veg}$ – Zgps) then this may introduce a systematic error to the DEMs given that there can be a time lag between sand-trapping and vegetation growth. For example, using a fixed value of vegetation height at the seasonal scale may cause areas of sand deposition to be under-estimated compared with areas of erosion (where both vegetation and sand are removed). The use of Zmin avoids this problem because it is determined at the time of the survey and changes across the DEM.

Decadal and seasonal variations in embryo dune field morphology

The short-term process experiments indicate that, having crossed the beach, onshore winds slow down as they reach the seaward side of the vegetated embryo dunes, suggesting any sediment in transport will be deposited causing dune accretion. This is consistent with studies of incipient foredunes on which vegetation traps blowing sand (Olivier and Garland, 2003; Anthony *et al.*, 2006; Delgado-Fernandez, 2011) and is a key process in the transformation from incipient to established foredunes (Hesp, 2002, 2011). However, because these embryo dunes have formed on the upper- and mid-beach rather than at the back of the beach or immediately seaward of the foredune, sediment transport can still occur from the upper beach to the established foredunes. Airflow speeds up to landward of the embryo dunes on the flat, unvegetated upper beach, with the potential for additional sediment entrainment, but then decelerates at the primary foredune toe. This suggests that whilst the embryo dunes may reduce the amount of sediment being transferred from the lower-mid beach to the main foredune, some sediment eroded from the upper beach (or from the embryo dunes themselves) could reach the established foredune. During offshore winds, there is limited evidence of flow separation taking place on the seaward side of the foredune, but flow deceleration does occur before wind velocities increase across the primary foredune toe and upper beach. In July 2010, direct offshore winds transported sediment across the main foredune and *c.* $9\,g\,m^{-1}\,h^{-1}$ of horizontal flux was recorded on the upper beach, despite a surface moisture content of nearly 20% (Figure 8). No sediment transport was recorded on the downwind (seaward) side of the embryo dunes indicating these dunes may have trapped and retained the blowing sand. Horizontal flux on the lower beach is likely to have been locally entrained. In contrast, under quite strong oblique offshore winds in January 2010 sediment transport was only recorded on the seaward side of the embryo dunes. This may be due to high surface moisture on the foredune and upper beach ($> 30\%$) limiting entrainment, whereas downwind surface moisture was variable and some sediment was trapped seaward of the embryo dunes suggesting these dunes may have been eroding.

These short-term experiments are limited in scope and wind speeds were generally low, however they suggest some general patterns of sediment movement that can help to interpret the changes in seasonal and decadal geomorphology. First, the embryo dunes can intercept sand being blown inland from the beach. However the gap between the embryo dunes and the foredunes, which is part of the upper beach and floods at high tide, is wide enough for flow attachment and sediment entrainment to take place. This maintains some sediment supply to the foredune. Second, under offshore winds, sediment may be transported from the foredunes to the embryo dunes across the upper beach. The experiments also have some implications for interpreting the relative importance of offshore and onshore winds for the development of the embryo dunes. The results need to be treated with some caution as flow patterns, particularly the occurrence of flow separation and reversal, may be different at higher wind speeds and under different approaching wind directions for different dune morphologies (Lynch *et al.*, 2010; Bauer *et al.*, 2012). Well-developed dunes are often associated with onshore winds. However, several recent studies have described coastal dune development where offshore winds play an important role. For example, where flow separation occurs the resulting near-surface reversed flow may be capable of transporting sand from the beach to the foredunes (Lynch *et al.*, 2009, 2010). On the Theddlethorpe dunes, during these experiments flow reversal did not take place during offshore winds. This is possibly due to a gentle slope, short foredune height and also low overall wind speeds. However, whilst wind velocities were slower over the established foredune than on the beach (due to high upwind surface roughness over the vegetated land), offshore winds were capable of sand transport on the seaward side of the foredune and wind speed recovered rapidly as it travelled over the upper beach (typically reaching 60–80% of wind speed on the mid-beach). The topography and vegetation cover of the embryo dunes is likely to slow these offshore winds, especially at the near surface. However, on the downwind side of the embryo dune field wind speeds are similar to, or slightly higher than those on the upper beach. This suggests that, at this site, whilst offshore winds of a given strength may have substantially less geomorphological impact than onshore winds with regards to the development of the foredune, offshore and onshore winds are likely to have a similar capacity (within *c.* 20%) when it comes to sediment delivery to the embryo dunes.

The lack of topographic data between the seasonal surveys makes it difficult to attribute geomorphological changes in the embryo dunes to the specific actions of wind and water. The changes in the dune field identified from the DEMs suggest that the embryo dunes are characterized by a classical seasonal cycle of summer accumulation and autumn–winter erosion, probably occurring during storm surge events. This has been previously observed for foredunes along sandy beaches (Sarre, 1989; Carter *et al.*, 1990; Arens, 1996; Ruz and Meur-Férec, 2004) where sediment removed during scarping by storm waves usually returns to the coastal dunes under fair conditions as a part of the recovery of the beach–dune system cycle (Carter *et al.*, 1990). The orientation and shape of the dunes clearly reflects the dominant winds prior to the acquisition of the TLS data. Following periods when onshore and offshore winds had similar potential sand transporting capacity the dunes showed no preferred orientation (e.g. January 2010). In contrast when winds from one direction dominated the dunes showed a clear preferred orientation (e.g. June 2010). The latter is visible in the summer 2010 aerial photograph shown in Figure 1c. It is, however, unclear whether the distinct corridors of erosion seen in January 2010 were formed by storm waves, strong winds or a combination of both.

The annual expansion of the field of embryo dunes from 2001 to 2007 suggests that none of the storm surge events identified was significant enough to completely destroy the dunes from one year to the next. The relative timing of aerial photograph acquisition (summer) and storm surges (typically winter) makes it impossible to know whether these storm events had any impact on the dunes, such as scarping, when they occurred. However if scarping and erosion did occur during the winter months, by the following summer the dunes had clearly recovered as there was no evidence of scarping on the aerial photographs, and the dune field expanded year-on-year. The early-mid part of this decade had a generally low incidence of severe storm surges compared with the 1990s and more recent years (Montreuil and Bullard, 2012) which would have increased the likelihood of the dune field becoming established both morphologically and in terms of the stabilizing vegetation cover. The high numbers of storm surges in 2007–2008 are probably the cause of the substantial reduction in area of the dune field between summer 2007 and summer 2008, although again no evidence of specific erosion features was visible on the aerial photographs. Few storm surges occurred in the last three years of the decade and the dune field expanded very rapidly. This accretion is unlikely to have been substantially influenced by changes in sediment supply linked to the intertidal bar migration and merging to the upper foreshore because at Theddlethorpe, intertidal bars migrate alongshore at a rate of up to 30 m per month in a southward direction (van Houwelingen *et al.*, 2006). Landward migration is not ubiquitous for low amplitude bars such as ridge-runnel bars (Houser, 2009) however the beachface and foreshore can provide a source of sand if the beach morphology is flattened through runnel infilling by swash (Anthony *et al.*, 2009), although that was not observed at Theddlethorpe.

A particular point of interest concerning the Theddlethorpe site is whether or not the dunes should still be considered embryo dunes, or whether they have become, or can perform the function of a foredune. From the DEM the patch of dunes is still very variable in terms of height, and clear corridors of erosion can be seen where storm events breach the dune field which is typical of embryo dunes, or incipient foredunes. However, the dune field in 2011 was 70 m wide and extended over 250 m alongshore acting as a potential barrier between the main landward established foredunes and the sea. Several studies have reported how embryo dunes can decrease sediment supply to the foredunes by trapping sand being transported onshore from the beach (Ruz and Allard, 1994; Kuriyama *et al.*, 2005; Millington *et al.*, 2008; Delgado-Fernandez, 2011) and a large area of dunes such as those in the present study might be expected to have a similar affect. However, at Theddlethorpe the foredunes and the embryo dunes are still separated by an unvegetated beach which floods at high tide and varies in width from 1 m to 40 m. As outlined earlier, this means the landward foredunes can still have an exchange of materials with the upper beach. The reason why these embryo dunes have formed on the mid-beach rather than adjacent to the foredunes may be due to the specific location of the dune field. The embryo dune field has developed on a slight change in orientation of the coastline which is oriented 325° to the north of the dunes and 342° to the south of the dunes. Alongshore winds blowing from the north can travel over >750 m of sandy beach before reaching the embryo dune field, and may provide a significant input of material to the dunes. The impact of such winds can clearly be seen in the 2010 aerial photograph in Figure 2 from the orientation and elongation of the dunes from NNW-SSE, particularly those on the seaward side of the dune field. Such alongshore winds can elongate embryo dune fields (e.g. Anthony *et al.*, 2006, 2007) and if they occur in combination with offshore winds, will slow the rate at which the embryo dunes merge with the foredunes.

On the Lincolnshire coast there is another variable to consider, which is that this is a rapidly accreting coastline. For several decades prior to the formation of the embryo dune field the foredunes at Theddlethorpe were prograding at an average rate of $>2\,m\,yr^{-1}$, but at times (e.g. 1976–1983) exceeding $3\,m\,yr^{-1}$ (Montreuil and Bullard, 2012). However, in 2005 foredune progradation at Theddlethorpe slowed to $<1\,m\,yr^{-1}$ and has continued at a similar, comparatively slow rate. This slowing down of the foredune advance coincides with the expansion of the embryo dunes on the upper and mid-beach. From 2005 to 2011 the mean annual reduction in the width of the gap between the foredunes and the embryo dunes has been $4.4\,m\,yr^{-1}$. It could be inferred that this rate of change reflects the combination of an average of *c.* $1\,m\,yr^{-1}$ advance of the foredunes and *c.* $3\,m\,yr^{-1}$ expansion of the embryo dunes. Given the mean gap size in 2011 was 26 m, at the current rate the embryo dunes and the foredunes will merge within the next decade, although this will not happen uniformly because the gap width is much narrower at the south of the study site (1 m) compared to the north (40 m). The time period over which this merger between the embryo dunes and foredunes could take place at Theddlethorpe (*c.* 20 years from embryo dune initiation) is of the same order of magnitude as has been reported elsewhere for the evolution of incipient foredunes into established foredunes. For example, 6–8 years in western Poland (Labuz, 2009), 10 years in south-eastern Australia (McLean and Shen, 2006), 20 years in eastern Hudson Bay, Canada (Ruz and Allard, 1994) and 50 years on Prince Edward Island, Canada (Mathew *et al.*, 2010). This variability in the time taken for established foredunes to develop reflects multiple inter-acting processes operating at a range of different timescales (summarized by Hesp, 2002) that are likely to be site-specific.

Conclusions

Sand supply is currently unlimited on the rapidly prograding north Lincolnshire coast; it is not clear precisely what triggered the formation of the patch of embryo dunes in 2001, however since inception, their morphological development over the last 10 years has been mainly controlled by the regional wind regime and the occurrence of major storm surge events. Aerial photographs have provided a useful indication of annual expansion of the dune field, and high resolution seasonal surveys using TLS have been shown to complement these data. TLS is a rapid and effective technique for obtaining three-dimensional topographic data of the embryo dunes provided that the impact of vegetation on any subsequently derived digital elevation model can be accounted for. Tests conducted at the Theddlethorpe field site suggest that minimum values within the TLS point cloud for a given size of grid cell (in this case 0.05 m × 0.05 m) provide an adequate approximation of the true ground surface. The use of minimum values works at this site because vegetation cover is less than 100% making it possible for the laser beam to reach the surface, or near-surface sufficiently often. In areas of more dense vegetation cover, or where vegetation structure is more complex than the grasses encountered in this study, the use of minimum values may not be appropriate and therefore it is recommended that site-specific tests are conducted before assuming that TLS data can be used to obtain topographic data for vegetated dunes. An advantage of using the Zmin approach is that even if there are substantial variations in vegetation height from season to season the filtered data are likely to reflect the ground surface topography. This is contingent on the assumptions that there is a temporally sustained significant relationship between $Zmin_{veg}$ and Zgps and that the canopy is partial. This avoids potential problems associated with any time lag between sand accretion and vegetation growth.

The seasonal changes in the dune field identified from the DEMs indicate that the embryo dunes are characterized by a classical seasonal cycle of summer accumulation and autumn–winter erosion occurring during storm surge events. Short-term process experiments suggest that both onshore and offshore winds contribute to the development of the embryo dunes at this site due to the gap between the established foredunes and the embryo dune field. Although the embryo dunes act as a potential barrier between the main landward established foredunes and the sea protecting them from storm surge erosion, the foredunes have continued to prograde over the past 10 years albeit at a slower rate (1 m h^{-1} since 2005 rather than 2 m yr^{-1} prior to 2005). This, and the measurements of airflow and sand transport, suggests that beach–dune interactions and active sediment exchange continue to occur in both the pre-existing foredunes and the embryo dunes on the beach. Even after 10 years of development, the embryo dunes on this site are still uneven in height and susceptible to regular erosion and the dune field morphology reflects the complex wind regime operating on this coastline.

Acknowledgements—This study was supported by a postgraduate research grant from the British Society for Geomorphology to ALM, and a small grant from the Centre for Hydrological and Ecosystem Science, Loughborough University to JEB and JM. The authors would like to thank Daniel Scott, Julian O'Neill, Joseph Pomeroy and Tom Matthews for field assistance in collecting the terrestrial laser scanner data. Special thanks are extended to all the Natural England staff at Saltfleetby-Theddlethorpe National Nature Reserve, especially Roger Briggs and John Walker.

References

Aagaard T, Davidson-Arnott R, Greenwood B, Nielsen J. 2004. Sediment supply from shoreface to dunes: linking sediment transport measurements and long-term morphological evolution. *Geomorphology* **60**: 205–224.

Allen TR, Oertel GF, Gares PA. 2012. Mapping coastal morphodynamics with geospatial techniques, Cape Henry, Virginia, USA. *Geomorphology* **137**: 138–149. DOI. 10.1016/j.geomorph.2010.10.040.

Anthony EJ, Ruz M-H, Vanhée S. 2009. Aeolian sand transport over complex intertidal bar-trough beach topography. *Geomorphology* **105**: 95–105.

Anthony EJ, Vanhée S, Ruz M-H. 2006. Short-term beach–dune sand budgets on the North Sea coast of France: sand supply from shoreface to dunes, and the role of wind and fetch. *Geomorphology* **81**: 316–329. DOI. 10.1016/j.geomorph.2006.04.022

Anthony EJ, Vanhée S, Ruz M-H. 2007. Embryo dune development on a large, actively accreting macrotidal beach: Calais, North Sea coast of France. *Earth Surface Processes and Landforms* **32**: 631–636. DOI. 10.1002/esp.1442.

Arens SM. 1994. Aeolian Processes in the Dutch Foredunes, PhD Thesis, University of Amsterdam.

Arens SM. 1996. Patterns of sand transport on vegetated foredunes. *Geomorphology* **17**: 339–350.

Bagnold RA. 1941. The Physics of Blown Sand and Desert Dunes. Methuen: London.

Bauer BO, Davidson-Arnott RGD, Walker IJ, Hesp PA, Ollerhead J. 2012. Wind direction and complex sediment transport response across a beach–dune system. *Earth Surface Processes and Landforms* **37**: 1661–1677.

Brooks SM, Spencer T. 2010. Temporal and spatial variations in recession rates and sediment release from soft rock cliffs, Suffolk coast, UK. *Geomorphology* **124**: 26–41. DOI. 10.1016/j.geomorph.2010.08.005

Bullard JE, Austin MJ. 2011. Dust generation on a proglacial floodplain, West Greenland. *Aeolian Research* **3**: 43–54.

Burrough PA, McDonnell RA. 1998. Principles of Geographical Information Systems, 2nd edition. Oxford University Press: New York.

Carter RGW. 1988. Coastal Environments. Academic Press: London.

Carter RGW, Hesp PA, Nordstrom KF. 1990. Erosional landforms in coastal dunes. In Coastal Dunes. Form and Process, Nordstrom K, Psuty N, Carter B (eds). John Wiley & Sons: Chichester; 217–250.

Chandler JH, Fryer JG, Jack A. 2005. Metric capabilities of low-cost digital cameras for close range surface measurement. *The Photogrammetric Record* **20**: 12–26. DOI. 10.1111/j.1477-9730.2005.00302

Coveney S, Fotheringham AS. 2011. Terrestrial laser scan error in the presence of dense ground vegetation. *The Photogrammetric Record* **26**: 307–324.

Davidson-Arnott RGD, Law MN. 1990. Seasonal patterns and controls on sediment supply to coastal foredunes, Long Point, Lake Erie. In Coastal Dunes: Form and Process, Nordstrom KF, Psuty NP, Carter RWG (eds). John Wiley & Sons: Chichester; 177–200.

Delgado-Fernandez I. 2011. Meso-scale modelling of aeolian sediment input to coastal dunes. *Geomorphology* **130**: 230–243. DOI. 10.1016/j.geomorph.2011.04.001

Estornell J, Ruiz LA, Hermosilla T. 2012. Assessment of factors affecting shrub volume estimations using airborne discrete-return LIDAR data in Mediterranean areas. *Journal of Applied Remote Sensing* **6**: 063544-1– 063544-10. DOI. 10.1117/1.JRS.6.063544

Floyd DA, Anderson JE. 1987. A comparison of three methods for estimating plant cover. *Journal of Ecology* **75**: 221–228.Fryrear DW. 1986. A field dust sampler. *Journal of Soil and Water Conservation* **41**: 117–120.

Gomes N, Andrade C, Roariz C. 1992. Sand transport rates in the Troia-Sines Arc, southwestern Portugal. In Coastal Dunes, Carter RWG, Curtis TGF, Sheehy-Skeffington MJ (eds). Balkema: Rotterdam; 33–41.

Guarnieri A, Vettore A, Pirotti F, Menenti M, Marani M. 2009. Retrieval of small-relief marsh morphology from terrestrial laser scanner, optimal spatial filtering and laser return intensity. *Geomorphology* **113**: 12–20. DOI. 10.1016/j.geomorph.2009.06.005

Hesp PA. 1983. Morphodynamics of incipient foredunes in New South Wales, Australia. In Eolian Sediments and Processes, Brookfield ME, Ahlbrandt TS (eds). Elsevier: Amsterdam; 325–342.

Hesp PA. 1989. A review of biological and geomorphological processes involved in the initiation and development of incipient foredunes. In Coastal Sand Dunes, Gimingham CH, Ritchie W, Willetts BB, Willis AJ (eds). Proceedings of the Royal Society of Edinburgh 96B. Royal Society: Edinburgh; 181–201.

Hesp PA. 2002. Foredunes and blowouts: initiation, geomorphology and dynamics. *Geomorphology* **48**: 245–268.

Hesp P. 2011. Dune coasts. In Treatise on Estuarine and Coastal Science, Wolanski E, McLusky DS (eds). Academic Press: Waltham, MA; vol. **3**, 193–221.

Hesp PA, Davidson-Arnott R, Walker IJ, Ollerhead J. 2005. Flow dynamics over a foredune at Prince Edward Island, Canada. *Geomorphology* **65**: 71–84.

Houser C 2009. Synchronization of transport and supply in beach–dune interaction. *Progress in Physical Geography* **33**: 733–746.

Houser C, Mathew S. 2011. Alongshore variation in foredune height in response to transport potential and sediment supply, South Padre Island, Texas. *Geomorphology* **125**: 62–72. DOI. 10.1016/j.geomorph.2010.07.028

Jackson PS, Hunt JCR. 1975. Turbulent wind flow over a low hill. *Quarterly Journal of the Royal Meteorological Society* **101**: 929–955.

Juraidi J, Wakae N, Kato S, Aoki S-I. 2010. Morphological monitoring of coastal dune using differential GPS and 3D terrestrial scanner. *Proceedings of the 5th International Conference on Asian and Pacific Coasts* **2**: 313–320.

Kuriyama Y, Mochizuki N, Nakashina T. 2005. Influence of vegetation on aeolian sand transport rate from a backshore to a foredune at Hasaki, Japan. *Sedimentology* **52**: 1123–1132.

Labuz TA. 2009. The increase of the coastal dune area of the Swina Gate Sandbar, west Polish coast. *Zeitschrift der Deutschen Gesellschaft für Geowissenschaften* **160**: 123–135.

Leggett DJ, Lowe JP, Cooper NJ. 1998. Beach evolution on the Southern Sea coast. *Coastal Engineering* **26**: 2759–2772.

L Geosystems. 2008. Leica ScanStation 2 User Manual. Leica: Switzerland.

Li ZL. 1988. On the measure of digital terrain model accuracy. *The Photogrammetric Record* **12**: 873–877.

Lynch K, Jackson DWT, Cooper JAG. 2009. Foredune accretion under offshore winds. *Geomorphology* **105**: 139–146.

Lynch K, Jackson DWT, Cooper JAG. 2010. Coastal foredune topography as a control on secondary airflow regimes under offshore winds. *Earth Surface Processes and Landforms* **35**: 344–353.

Mathew S, Davidson-Arnott RGD, Ollerhead J. 2010. Evolution of a beach–dune system following a catastrophic storm overwashing event: Greenwich Dunes, Prince Edward Island, 1936–2005. *Canadian Journal of Earth Sciences* **47**: 273–290 DOI. 10.1139/E09-078

McLean R, Shen J-S. 2006. From foreshore to foredune: foredune development over the last 30 years at Moruya Beach, New South Wales, Australia. *Journal of Coastal Research* **22**: 28–36.

Millington JA, Fullen MA, Moore GM, Booth CA, Trueman IC, Worsley AT, Richardson N. 2008. Morphodynamics of the Morfa Dyffryn coastal dunes, mid-Wales: photographic survey 1988–2007. In Environmental Problems in Coastal Regions VII, Brebbia CA (eds), WIT Transactions on the Built Environment 99. WIT Press: Southampton; 211–220.

Montreuil A-L. 2012. *Aeolian Dune Development and Evolution on a Macro-tidal Coast with a Complex Wind Regime, Lincolnshire Coast, UK*, PhD Thesis, Loughborough University, UK.

Montreuil A-L, Bullard JE. 2010. Using high resolution ground survey and LIDAR data to monitor embryo dune development in a conservation area, North Lincolnshire (UK). In European Association of Remote Sensing Laboratories Symposium, 30th Symposium. UNESCO: Paris; 457–461.

Montreuil A-L, Bullard JE. 2012. A 150 year record of coastline dynamics within a large-scale sediment cell: eastern England. *Geomorphology* **179**: 168–185.

Nagihara S, Mulligan KR, Xiong W. 2004. Use of a three-dimensional laser scanner to digitally capture the topography of sand dunes in high spatial resolution. *Earth Surface Processes and Landforms* **29**: 391–398 DOI. 10.1002/esp.1026

Olivier MJ, Garland GG. 2003. Short-term monitoring of foredune formation on the east coast of south Africa. *Earth Surface Processes and Landforms* **28**: 1143–1155. DOI. 10.1002/esp.549

Petersen PS, Hilton MJ, Wakes SJ. 2011. Evidence of aeolian sediment transport across an Ammophila arenaria-dominated foredune, Mason Bay, Stewart Island. *New Zealand Geographer* **67**: 174–189.

Pye K 1983. Coastal dunes. *Progress in Physical Geography* **7**: 531–557.

Pye K, Blott SJ. 2008. Decadal-scale variation in dune erosion and accretion rates: an investigation of the significance of changing storm tide frequency and magnitude on the Sefton coast. *Geomorphology* **102**: 652–666. DOI. 10.1016/j.geomorph.2008.06.011

Rango A, Chopping M, Ritchie J, Havstad K, Kustas W, Schmugge T. 2000. Morphological characteristics of shrub coppice dunes in desert grasslands of southern New Mexico derived from scanning LIDAR. *Remote Sensing of Environment* **74**: 26–44.

Robinson AHW, 1964. The inshore waters, sediment supply and coastal changes of part of Lincolnshire. *East Midland Geographer* **3**: 307–321.

Rosser NJ, Petley DN, Lim M, Dunning SA, Allison RJ. 2005. Terrestrial laser scanning for monitoring the process of hard rock coastal cliff erosion. *Quarterly Journal of Engineering Geology & Hydrogeology* **38**: 363–375.

Rosso PH, Ustin SL, Hastings A. 2006. Use of lidar to study changes associated with Spartina invasion in San Francisco Bay marshes. *Remote Sensing of Environment* **100**: 295–306.

Ruz MH, Allard M. 1994. Foredune development along a sub-arctic emerging coastline, eastern Hudson Bay, Canada. *Marine Geology* **117**: 57–74.

Ruz, MH, Meur-Férec C. 2004. Influence of high water levels on aeolian sand transport: upper beach/dune evolution on a macrotidal coast, Wissant Bay, northern France. *Geomorphology* **60**: 73–87. DOI. 10.1016/j.geomorph.2003.07.011

Sarre RD. 1989. The morphological significance of vegetation and relief on coastal foredune processes. *Zeitschrift für Geomorphologie* **73**: 17–31.

Saye SE, van der Wal D, Pye K, Blott SJ. 2005. Beach–dune morphological relationships and erosion/accretion: an investigation at five sites in England and Wales using LIDAR data. *Geomorphology* **72**: 128–155. DOI. 10.1016/j.geomorph.2005.05.007

Schmid KA, Hadle BC, Wijekoon N. 2011. Vertical accuracy and use of topographic LIDAR data in coastal marshes. *Journal of Coastal Research* **27**: 116–132.

Shao Y, McTainsh GH, Leys JF, Raupach MR. 1993. Efficiencies of sediment samplers for wind erosion measurement. *Australian Journal of Soil Research* **31**: 519–532.

Sherman DJ, Bauer BO. 1993. Dynamics of beach–dune systems. *Progress in Physical Geography* **17**: 413–447.

Soudarissanane S, Lindenbergh R, Menenti M, Teunisse P. 2011. Scanning geometry: influencing factor on the quality of terrestrial laser scanning points. *Journal of Photogrammetry and Remote Sensing* **66**: 389–399.

Stout JE, Zobeck TM. 1996. Establishing the threshold condition for soil movement in wind-eroding fields. Proceedings of the International Conference on Air Pollution from Agricultural Operations. MWPS C-3 Kansas City, 7–9 February; 65–71.

Suanez S, Cariolet J-M, Cancouët R, Ardhuin F, Delacourt C. 2012. Dune recovery after storm erosion on a high-energy beach: Vougot Beach, Brittany (France). *Geomorphology* **139–140**: 16–33. DOI. 10.1016/j.geomorph.2011.10.014

Thieler ER, Himmelstoss EA, Zichichi JL, Ergul A. 2009. *Digital Shoreline Analysis System (DSAS) Version 4.0 — an ArcGIS Extension for Calculating Shoreline Change*, US Geological Survey Open-file Report 2008–1278. US Geological Survey: Reston, VA. http://pubs.usgs.gov/of/2008/1278/

van Houwelingen S, Masselink G, Bullard J. 2006. Characteristics and dynamics of multiple intertidal bars, North Lincolnshire, England. *Earth Surface Processes and Landforms* **31**: 428–44. DOI. 10.1002/esp.1276

van Tooren BF, Schat H, ter Borg SJ. 1983. Succession and fluctuation in the vegetation of a Dutch beach plain. *Vegetatio* **53**: 139–151.

Wang C, Menenti M, Stoll M-P, Feola A, Belluco MM. 2009. Separation of ground and low vegetation signatures in LIDAR measurements of

salt-marsh environments. *IEEE Transactions on Geoscience and Remote Sensing* **47**: 2014–2023.

Weligepolage K, Gieske ASM, Su Z. 2012. Surface roughness analysis of a conifer forest canopy with airborne and terrestrial laser scanning techniques. *International Journal of Applied Earth Observation and Geoinformation* **14**: 192–203.

Wiggs GFS, Bullard JE, Garvey B, Castro I. 2002. Interactions between airflow and valley topography with implications for aeolian sediment transport. *Physical Geography* **21**: 366–380.

Young AP, Asford SA. 2006. Application of airborne LIDAR for seacliff volumetric change and beach-sediment budget contributions. *Journal of Coastal Research* **22**: 307–318.